DISCIPLINARUM SCIENTIA *Disciplinarum Scientia.* **Série: Naturais e Tecnológicas**
Santa Maria, v. 27, n. 3, p. 245-268, 2026
Recebido em: 20.07.2026. Aprovado em: 23.09.2026.
ISSN 2176-462X | DOI: doi.org/10.37779/nt.v27i3.5893

# DEVELOPMENT AND BIOLOGICAL EVALUATION OF A NANOFORMULATION CONTAINING OLIVE LEAF EXTRACT AND OLIVE OIL[1]

## *DESENVOLVIMENTO E AVALIAÇÃO BIOLÓGICA DE UMA NANOFORMULAÇÃO CONTENDO EXTRATO DE FOLHAS DE OLIVEIRA E AZEITE DE OLIVA[1]*

**Larissa da Silva Silveira[2], Elisandra da Silva Pena da Fonseca[2], Walter Paixão de Sousa Filho[2], Mateus Cláudio Zinhani[2], Rodrigo Montezano da Cunha[2], Aline Rossato[2], Carolina Rapachi Fortes[2], Klynsman Gambini Dornelles[3], Francielle Liz Monteiro[3], Luiz Fernando Rodrigues Júnior[2], Liana da Silva Fernandes[2] e Michele Rorato Sagrillo[2]**

**ABSTRACT**

Given the growing increase in agro-industrial waste generation within olive cultivation considering that Rio Grande do Sul is among the largest olive oil producers in Brazil the valorization of such by-products, particularly olive leaves, is proposed through biotechnological application using nanostructured systems. This initiative aligns with the principles of the circular economy, combining sustainability and innovation. A nanoemulsion containing olive leaf extract combined with olive oil (NEAZ) was developed and evaluated according to its physicochemical characteristics, stability tests, and *in vitro* biocompatibility in two cell models, Peripheral blood mononuclear cells (PBMCs) and immortalized human keratinocytes (HaCaT). The developed nanoemulsion presented suitable physicochemical characteristics, as evidenced by its nanometric average size, low polydispersity, and a zeta potential compatible with system stability. In the biological assays, the treatments demonstrated high biocompatibility, with low cytotoxicity, stimulation of cell proliferation, and, under certain conditions, a cytoprotective effect. Furthermore, relevant antioxidant activity was observed, reinforcing the biological potential of the formulation. Thus, bioactive compounds obtained from olive waste, especially when incorporated into nanoemulsions and combined with olive oil, stand out as an innovative strategy for the valorization of agro-industrial by-products.

**Keywords:** Sustainability; *Olea europaea* L; circular economy; social responsibility.

---

1 Part of the doctoral thesis presented to the Graduate Program in Nanosciences, Universidade Franciscana - UFN, Santa Maria, RS, Brazil.

2 Graduate Program in Nanosciences, Universidade Franciscana - UFN, Santa Maria, RS, Brazil. E-mail: larissa.silveira@ufn.edu.br. ORCID: https://orcid.org/0000-0003-4460-9857; E-mail: elisandrapena@ufn.edu.br. ORCID: https://orcid.org/0009-0007-1025-699X; E-mail: walter.paixao@ufn.edu.br. ORCID: https://orcid.org/0000-0001-5962-4908; E-mail: mateus.zinhani@ufn.edu.br. ORCID: https://orcid.org/0000-0003-1829-7546; E-mail: rodrigomontezano@ufn.edu.br. ORCID: https://orcid.org/0000-0003-0278-3566; E-mail: aline.rossato@ufn.edu.br. ORCID: https://orcid.org/0000-0001-6464-6255; E-mail: carolinarapachi@ufn.edu.br. ORCID: https://orcid.org/0009-0001-2356-025X; E-mail: luiz.fernando@ufn.edu.br. ORCID: https://orcid.org/0000-0001-7007-7431; E-mail: liana@ufn.edu.br. ORCID: https://orcid.org/0000-0003-4745-7617; E-mail: sagrillomr@ufn.edu.br. ORCID: https://orcid.org/0000-0001-5659-159X

3 Undergraduate degree in Biomedical Science from Universidade Franciscana (UFN), Santa Maria, Brazil. E-mail: k.dornelles@ufn.edu.br. ORCID: https://orcid.org/0009-0004-8980-2049; E-mail: francielle.monteiro@ufn.edu.br. ORCID: https://orcid.org/0000-0002-4698-9657

***RESUMO***

*Diante do crescente aumento da geração de resíduos agroindustriais na olivicultura, visto que o Rio Grande do Sul está entre os maiores produtores de azeite de oliva no Brasil, propõe-se a valorização de tais subprodutos, especialmente folhas de oliveira, com a aplica*ção *biotecnológica por meio de sistemas nanoestruturados, iniciativa essa, focada aos princípios da economia circular, associando sustentabilidade e inovação. Foi desenvolvida uma nanoemulsão contendo extrato de folhas de oliveira associado ao azeite de oliva (NEAZ) e avaliada segundo características* físico-químicas, testes de estabilidade *e avaliação de biocompatibilidade in vitro em dois modelos celulares, Células mononucleares do sangue periférico (PBMCs) e queratinócitos humanos imortalizados (HaCaT). A nanoemulsão desenvolvida apresentou características físico-químicas adequadas, evidenciadas pelo tamanho médio em escala nanométrica (121,6 nm), baixa polidispersão (0,203) e potencial zeta compatível com a estabilidade do sistema (-26,2 mV). Nos ensaios biológicos, os tratamentos demonstraram elevada biocompatibilidade, com baixa citotoxicidade, estímulo à proliferação celular e, em determinadas condições, efeito citoprotetor. Além disso, foi observada relevante atividade antioxidante, reforçando o potencial biológico da formulação. Dessa forma, os bioativos obtidos de resíduos da oliveira, especialmente quando incorporados em nanoemulsões e associados ao azeite de oliva, destacam-se como uma estratégia inovadora para a valorização de subprodutos agroindustriais.*

***Palavras-chave:*** *sustentabilidade; Olea europaea L.; economia circular; responsabilidade social.*

## 1 INTRODUCTION

In Brazil, olive cultivation has gained prominence, especially in the state of Rio Grande do Sul, where favorable climatic conditions in the southern regions favor the cultivation of olive trees. Consequently, the expansion of the productive chain directly implies a significant generation of agro-industrial waste. During the mechanical extraction of olive oil, by-products such as olive pomace, olive cake, or *sansa* are produced, composed of skin, pulp, and pit, in addition to containing residual oil. Concurrently, agricultural practices such as pruning result in the accumulation of leaves and branches. These materials present a high concentration of bioactive compounds responsible for the functional properties of both the fruits and the olive oil (Costa, 2019; Ferreira, 2024; Rodrigues *et al*., 2024).

The accumulation of this waste represents a major environmental challenge due to its high volume, with olive pomace accounting for approximately 80% of the product resulting from extraction, while leaves can reach up to 40 tons per year. When accumulated in large quantities, potentially toxic compounds, such as phenolics, can affect terrestrial microorganisms and contribute to the contamination of rivers and springs. Furthermore, the presence of volatile compounds and inorganic substances that are difficult to degrade favors the persistence of this waste in the environment, worsening its ecological impact (Rapacki, 2022; Nunes *et al*., 2019).

In this context, the valorization of this waste emerges as a fundamental strategy within the principles of the circular economy, based on transforming this environmental liability into a high value-added economic asset, aiming to maximize resource utilization and minimize waste generation. Reinserting these by-products into the productive chain not only reduces environmental impacts but

also adds economic value, transforming waste into strategic inputs. This approach promotes innovation, sustainability, and greater market competitiveness (Pennisi *et al*., 2023).

Olive leaves stand out among the by-products of the productive chain because they contain high concentrations of phenolic compounds, including oleuropein, hydroxytyrosol, luteolin, and verbascoside molecules associated with antioxidant, anti-inflammatory, and bioprotective properties. Due to these characteristics, the use of these compounds has aroused growing interest for pharmaceutical, cosmetic, and biotechnological applications. The phenolic composition of the olive tree, according to Nascimento (2025), is extremely complex, and many of its components have not yet been fully identified. The main compounds found in the leaves and fruits are oleuropeosides (such as oleuropein and verbascoside), flavonoids (flavones and flavonols), and simple phenols, such as tyrosol, hydroxytyrosol, and various phenolic acids, including caffeic, vanillic, syringic, coumaric, and protocatechuic acids molecules associated with antioxidant, anti-inflammatory, and bioprotective properties. Due to these characteristics, the use of these compounds has aroused growing interest for pharmaceutical, cosmetic, and biotechnological applications (Mello and Pinheiro, 2012).

Although they present high biological potential, these compounds have their technological application limited by chemical instability, oxidative degradation, low solubility, and reduced bioavailability. To circumvent these limitations, nanostructured systems emerge as alternatives to protect bioactives, increase their stability, and optimize their biological response. Nanotechnology provides controlled and targeted release of the active ingredient, vectorization to specific targets, and increased permeability across biological barriers through the incorporation of hydrophilic or hydrophobic molecules. Furthermore, it stands out for its low toxicity, absence of organic solvents in production, and ease of scaling. Generally obtained from biodegradable and biocompatible matrices, these nanocarriers are widely accepted for medical and pharmaceutical use, exhibiting toxicity up to 100 times lower than that of conventional polymeric particles. Nanoemulsions stand out among nanostructured systems due to their high surface area, ease of preparation, capacity to incorporate lipophilic and hydrophilic compounds, and potential for pharmaceutical and cosmetic applications. Additionally, these systems can favor the stability of bioactive compounds and improve their biological performance (Fathia *et al*., 2012).

Given this context, the present study aimed to develop a nanoformulation containing olive leaf extract combined with olive oil, characterize it regarding its physicochemical properties and stability, and evaluate its *in vitro* biocompatibility in peripheral blood mononuclear cells and human keratinocytes.

## 2 METHODOLOGY

### 2.1 COLLECTION OF OLIVE CULTIVARS AND PREPARATION OF THE HYDROALCOHOLIC EXTRACT OF THE LEAVES

Green leaves from different cultivars of *Olea europaea* L. (Arbosana, Arbequina, Koroneiki, and Coratina) were collected from an olive grove located in the municipality of Caçapava do Sul, Rio Grande do Sul, Brazil. Botanical identification of the cultivars was performed based on the analysis of morphological characteristics, associated with local agronomic knowledge, and representative samples of each cultivar were deposited in the SMDB Herbarium (Santa Maria - Department of Biology) jardim botânico at the Federal University of Santa Maria (UFSM).

The extract was prepared following the methodology described in patent registration BR 102023015892-7, which comprises the following steps: the plant material was initially air-dried at room temperature. Subsequently, the leaves were ground using an electric knife mill until a homogeneous powder was obtained. Thereafter, 150 g of the ground plant material were transferred to amber glass bottles containing 500 mL of 70% (v/v) ethanol, establishing an extraction ratio of 1:3.3 (w/v). The extraction process was carried out by static maceration for seven days at room temperature and protected from light. After the extraction period, the mixture was filtered through a filter with an approximate pore size of 25 µm, and the solvent was removed under reduced pressure (approximately 17 hPa) using a Yamato RE801 rotary evaporator operating at 40 °C and 80 rpm. The resulting hydroalcoholic extract was stored in amber glass containers and kept protected from light until use.

### 2.2 PREPARATION, CHARACTERIZATION, AND STABILITY OF THE NANOEMULSION

#### 2.2.1 Preparation of the Nanoformulation

A nanoemulsion containing a hydroalcoholic extract of olive leaves was prepared using the phase inversion technique, which is based on the transition between oil-in-water (O/W) emulsions, promoted by surfactant reorganization and the energy conditions applied to the system, favoring the formation of nanometer-scale droplets.

The aqueous phase consisted of polysorbate 80 (Tween®) (0.8% w/v) and Milli-Q® water (54% v/v). The oil phase was composed of sorbitan monostearate (Span® 80) (0.8% w/v), hydroalcoholic olive leaf extract (20% v/v), ethanol (6.8% v/v), and olive oil (0.8% w/v).

Both phases were previously heated to approximately 50 °C in a water bath under magnetic stirring for 10 min. Subsequently, the extract was incorporated into the system, and stirring was

maintained for an additional 5 min. Thereafter, the aqueous phase (maintained in an ice bath) was transferred to an Ultra-Turrax® homogenizer and stirred at 10,000 rpm for 10 min. After this period, the oil phase was poured into the aqueous phase under continuous stirring, promoting the formation of the final emulsion. The nanoemulsion was then subjected to high-speed homogenization using an Ultra-Turrax® at 17,000 rpm for 40 minutes, while maintained in an ice bath to prevent degradation of the active ingredients due to excessive heating; this shearing step characterizes a high-energy process. Finally, the organic solvent was removed by rotary evaporation at 40 °C and 80 rpm using a Yamato RE 801 rotary evaporator.

### 2.2.2 Characterization of the Nanoformulation and Stability Analysis

The nanoformulation was characterized by evaluating pH, polydispersity index (PDI), particle size, and zeta potential (ZP). Stability was assessed over a 90-day period under different storage conditions: clear glass vials exposed to light, amber glass vials protected from light, amber glass vials stored in a climate chamber at 35 ± 1 °C (ranging from 34 °C to 36 °C), and amber glass vials kept under refrigeration at -2 ± 1 °C (ranging from -1 °C to -3 °C). For stability analysis, samples were prepared and maintained under all described conditions in triplicate. Every 15 or 30 days, each sample was characterized to monitor the parameters over time. Particle diameter and polydispersity index were determined by dynamic light scattering (DLS) using a Zetasizer® Nano ZS instrument (ZEN 3600, Malvern Instruments) after diluting the dispersions in water (500-fold dilution, v/v). Results were expressed in nanometers (nm). Zeta potential was determined via electrophoretic mobility using a Zetasizer® Nano ZS (ZEN 3600, Malvern Instruments) after diluting the dispersions in a 10 mM NaCl solution (500-fold dilution, v/v) that had been pre-filtered through a 0.45 µm membrane. Results were expressed in millivolts (mV) as the mean of three determinations performed on separate suspensions. pH was measured using a properly calibrated potentiometer (DM-22, Digimed®), and all analyses were performed in triplicate (Godoi *et al*., 2025).

## 2.3 *IN VITRO* BIOCOMPATIBILITY ANALYSIS OF THE NANOEMULSION CONTAINING OLIVE LEAF EXTRACT AND OLIVE OIL

The biocompatibility analysis was performed using two distinct cellular models to ensure the safety and functionality of the active compounds during tissue repair. The use of Peripheral Blood Mononuclear Cells (PBMCs) is justified by the need to monitor the initial immune response, as these cells are among the first to interact with external agents and coordinate the inflammatory cascade essential for wound healing. In parallel, the use of the human keratinocyte cell line (HaCaT) is justified by its ability to mimic the primary cellular barrier of the epidermis. As re-epithelialization is a

critical and final stage of tissue repair, evaluating the behavior of these cells in response to the active compounds allows the assessment of key wound-healing parameters, such as cell viability and cell proliferation. Thus, the combination of both cellular models (PBMCs and HaCaT) enables a robust and integrated analysis, encompassing the modulation of the initial inflammatory response through to the effective reconstruction and closure of the skin barrier (Silva, 2025)

### 2.3.1 Peripheral Blood Mononuclear Cells (PBMCs)

Peripheral Blood Mononuclear Cells (PBMCs) derived from whole blood samples discarded from healthy adults were obtained from the Clinical Analysis Teaching Laboratory of the Franciscan University (LEAC-UFN) (experimental protocol approved by the UFN Human Research Ethics Committee) (CAAE number: 44940821.3.0000.5306), with the absence of identifying data.

Blood samples were processed for PBMC separation using a procedure based on density gradient centrifugation with Ficoll Histopaque 1077® reagent (Sigma-Aldrich). After blood was slowly layered onto the reagent (1:1 v/v), the samples were centrifuged for 30 min at 1000 rpm. Subsequently, the leukocyte layer was collected and transferred to Falcon-type tubes containing RPMI 1640 medium (Sigma-Aldrich) at a 1:1 (v/v) ratio. The mixture was then centrifuged for 10 min at 1000 rpm. After centrifugation, the supernatant was discarded, leaving only the cell pellet, which was resuspended in approximately 4 mL of RPMI 1640 cell culture medium (Sigma-Aldrich). Finally, cell counting was performed using a Neubauer chamber. PBMCs were seeded into 96-well plates containing RPMI 1640 cell culture medium (Sigma-Aldrich) supplemented with 10% fetal bovine serum and 1% antibiotics. Cells were cultured at a concentration of $2 \times 10^5$ cells $mL^{-1}$ per well (Riedhammer; Halbritter; Weissert, 2015). Subsequently, the cells were treated with the nanoemulsion containing the combined olive leaf extract and olive oil.

The treatments were performed in triplicate to ensure consistent statistical analysis. Hydrogen peroxide ($H_2O_2$) at 200 µM was used as a positive control for all assays, except for nitric oxide, for which sodium nitroprusside at 50 µM was used as the positive control.

### 2.3.2 Human Keratinocyte Cells (HaCaT)

These cells were cultured in Dulbecco's Modified Eagle Medium (DMEM) supplemented with 10% fetal bovine serum (FBS), 1% antibiotics consisting of penicillin (100 U/mL) and streptomycin (100 µg/mL), and the antifungal agent amphotericin (100 U/mL). Cells were maintained at 37 °C in a controlled atmosphere incubator containing 5% $CO_2$ and adequate relative humidity. The culture medium was renewed every 2-3 days to maintain optimal growth conditions. Cell culture was periodically monitored by microscopy to evaluate morphology and confluence until the criteria required for the

experimental assays were met. When confluence reached approximately 80-90%, cells were subcultured by dissociation with trypsin-EDTA solution.

Cells were seeded into 96-well plates ($5 \times 10^4$ cells $mL^{-1}$). After 24 h of incubation (37 ± 2 °C with 5% $CO_2$), the supernatant was removed, and 100 µL of the treatments were added. Treatments were performed using the nanoemulsion containing olive leaf extract and olive oil. The positive control consisted of hydrogen peroxide ($H_2O_2$, 100 µmol $L^{-1}$, 30% solution, Sigma-Aldrich®) and sodium nitroprusside dihydrate ($Na_2[Fe(CN)_5NO]\cdot 2H_2O$, 100 µmol $L^{-1}$, ACS reagent, ≥99%, Sigma-Aldrich®), whereas the negative control consisted of cells maintained only with culture medium. Eight replicates of each concentration and controls were performed on each plate. After treatment distribution, the plates were incubated (37 ± 2 °C with 5% $CO_2$) for 24 h and 72 h.

For both cell lines, cell viability and proliferation were evaluated using the MTT assay (3-(4,5-dimethylthiazol-2-yl)-2,5-diphenyltetrazolium bromide), following the instructions of Mosmann, (1983) and Alves *et al*., (2026). This colorimetric assay uses the MTT reagent, a yellow water-soluble tetrazolium salt that penetrates cells and is metabolized by mitochondrial enzymes in viable cells, forming violet-colored, water-insoluble formazan crystals that accumulate in the cellular cytoplasm. These crystals are solubilized by the addition of DMSO (dimethyl sulfoxide). After treatment, PBS (1X phosphate-buffered saline, pH 7.4) was added to the cells at a volume corresponding to the same amount of supernatant removed for the other assays, generally 110 µL, followed by the addition of 20 µL of MTT reagent at a concentration of 5 mg $mL^{-1}$ diluted in PBS (1X phosphate buffer, pH 7.4). The plates were protected from light, homogenized, and incubated in an oven at 37 °C with 5% $CO_2$ for 2 h. After this period, the supernatant was removed, and the cells were resuspended in 200 µL of DMSO. Absorbance measurements were performed using a Synergy HTX multimode microplate reader (BioTek Instruments, Inc., Winooski, VT, USA), controlled by Gen5 software (BioTek) at 570 nm, and the determination of cytotoxic potential was calculated relative to the negative control.

To determine the total rate of free radicals, the reagent 2′,7′-dichlorofluorescein diacetate (DCFH-DA) was used. This reagent can cross the cell membrane and is deacetylated by mitochondrial enzymes, generating 2′,7′-dichlorodihydrofluorescein, which reacts with reactive oxygen species (ROS), mainly hydrogen peroxide ($H_2O_2$), producing 2′,7′-dichlorofluorescein, which emits fluorescence. After completion of the incubation period of cells with the treatments, 50 µL of the supernatant were added to a black plate to avoid direct light exposure, together with 65 µL of TRIS buffer (pH 7.4) and 10 µL of dichloro working solution (0.1 mM), followed by incubation at room temperature for 1 h. Fluorescence was determined using a Synergy HTX multimode microplate reader (BioTek Instruments, Inc., Winooski, VT, USA), controlled by Gen5 software (BioTek), based on excitation and emission wavelengths of 488 nm and 525 nm, respectively.

To complement the determination of cell viability and genotoxic potential, a fluorometric assay was performed to quantify free DNA in the culture medium using the DNA-PicoGreen® reagent

(Invitrogen, Life Technologies), a fluorescent dye that binds to double-stranded DNA. To determine the presence of double-stranded DNA in the medium in which the cells were treated, due to possible cell disruption and cell death, 10 µL of the culture medium supernatant from treated cells, 80 µL of 1X TE buffer, and 10 µL of PicoGreen® reagent were added to a black 96-well plate and incubated for 5 min at room temperature. Fluorescence was measured using a Synergy HTX multimode microplate reader (BioTek Instruments, Inc., Winooski, VT, USA), controlled by Gen5 software (BioTek), at excitation and emission wavelengths of 480 nm and 520 nm, respectively (Sagrillo *et al.*, 2015).

The nitric oxide assay detects the presence of organic nitrite in the sample. Nitrite is detected and analyzed through the formation of a pink coloration when the Griess reagent is added to the sample containing $NO^-$. The sulfanilamide present in the Griess reagent is responsible for the formation of diazonium salts from nitrite in the sample. When the azo compound (N-1-naphthylenediamine dihydrochloride) interacts with the diazonium salts, a pink coloration develops in the sample.

## 3 RESULTS AND DISCUSSION

### 3.1 COLLECTION OF OLIVE CULTIVARS AND PREPARATION OF THE HYDROALCOHOLIC LEAF EXTRACT

The leaves used in the present study were obtained from an olive grove located in the municipality of Caçapava do Sul, Rio Grande do Sul, Brazil. Green leaves from different *Olea europaea* L. cultivars, including Arbosana, Arbequina, Koroneiki, and Coratina, were collected. Botanical identity was confirmed through the evaluation of morphological characteristics combined with local agronomic knowledge. Voucher specimens of each cultivar were deposited in the SMDB Herbarium of the Federal University of Santa Maria (UFSM), Santa Maria, Rio Grande do Sul, Brazil, under accession numbers SMDB 26078 (Arbosana), SMDB 26079 (Arbequina), SMDB 26080 (Koroneiki), and SMDB 26081 (Coratina).

### 3.2 PREPARATION, CHARACTERIZATION, AND STABILITY OF THE NANOEMULSION

#### 3.2.1 Preparation of the Nanoformulation

The preparation of the nanoemulsion containing olive leaf extract combined with olive oil (NEAZ) demonstrated the feasibility of the simultaneous incorporation of these components into a stable nanostructured system. The formulation exhibited a homogeneous macroscopic appearance, with a slightly opalescent, milky aspect and no evidence of phase separation during the initial observation period, indicating the successful formation of a stable colloidal system (Figure 1).

The two phases were not visually discernible during the evaluation, and no phase separation was observed in the formulation. The absence of an interface between the phases indicates that the system remained homogeneous, constituting an indication of its physical stability under the evaluated conditions.

**Figure 1 -** Macroscopic appearance of the nanoemulsion containing olive leaf extract and olive oil.



**Source**: Author's construction.

The visual stability observed is consistent with oil-in-water nanoemulsified systems, in which the reduced droplet size contributes to the uniform dispersion of the oil phase. These findings corroborate the formation of an appropriate nanostructure, even considering the complexity of the lipid composition employed (Perissinato, 2019; Azeredo, 2023).

From a processing standpoint, the obtainment of NEAZ required the application of high energy, with the use of Ultra-Turrax® homogenization being necessary, indicating greater resistance to the formation of droplets at the nanometric scale. This behavior can be attributed to the composition of olive oil, characterized by a high concentration of monounsaturated fatty acids, especially oleic acid, in addition to minor compounds, such as phenolics and tocopherols, which may interfere with the interfacial organization of surfactants. Consequently, there is greater difficulty in spontaneous phase inversion, requiring a higher energy input for system stabilization (Graván *et al.*, 2023). Although the literature widely describes the incorporation of olive leaf extracts into nanostructured systems, the use of olive oil as a lipid phase associated with this extract remains poorly explored. In this context, the present formulation differs by integrating two bioactive components derived from the same plant species, *Olea europaea* L., constituting an innovative approach in the development of nanostructured systems.

Furthermore, the association between olive leaf extract, an olive cultivation by-product, and olive oil promotes the integral utilization of the production chain, aligning with the principles of the circular economy and the valorization of agro-industrial residues. This strategy enables the

development of multifunctional systems rich in bioactive compounds, such as oleuropein, hydroxytyrosol, and essential fatty acids, which may act synergistically. From a biological perspective, organization at the nanometric scale may enhance the bioavailability and skin permeation of these compounds due to the high surface area and greater interaction with biological structures. Thus, NEAZ presents promising potential for dermatological applications, particularly in inflammatory conditions and those associated with oxidative stress (Pierre, 2024). Overall, the results indicate that the composition of the oil phase directly influences both the preparation method and the physicochemical characteristics of the system, being a determining factor in the development of nanoemulsions based on natural compounds.

### 3.2.2 Characterization of the nanoformulation and stability analysis

Initially, the characterization revealed a relatively homogeneous particle size distribution, with a polydispersity index (PDI) of 0.203, indicating a narrow particle size distribution. The PDI is an important parameter for evaluating the homogeneity of nanoparticulate systems, with lower values generally indicating greater uniformity in particle size (Patravale, Dandekar, and Jain, 2012). This result suggests adequate uniformity in droplet size, which may contribute to the kinetic stability of the nanoemulsion.

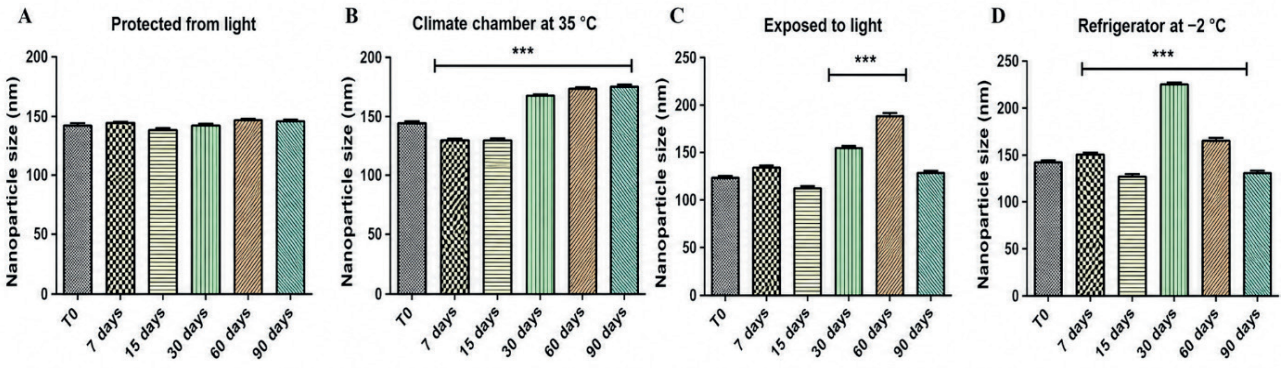
The mean droplet size of 121.6 nm confirms the formation of a nanoscale system (Figure 2), an important characteristic of oil-in-water nanoemulsions. The nanoscale droplet size provides a high interfacial area and may contribute to the physical stability of the system by reducing the tendency toward gravitational separation and other destabilization processes. In addition, the zeta potential of -26.2 mV indicates the presence of electrostatic repulsion between droplets, which may contribute to reducing their tendency to aggregate and, consequently, to maintaining the physical stability of the nanoemulsion (Patravale, Dandekar, and Jain, 2012).

The pH in the range of 4 - 5 remained compatible with systems containing phenolic compounds and with dermatological applications, not indicating a risk of significant chemical instability during the evaluated period.

The stability analysis of the nanoformulations over 60 days, under different storage conditions, allowed the evaluation of the system's robustness against temperature variations and light exposure. Overall, the absence of sedimentation and phase separation in macroscopic analyses indicates good physical stability of the formulation, regardless of the tested conditions. The maintenance of these parameters over time reinforces that the formulation composition and preparation method were suitable for obtaining a stable system. As described in the literature, variations in particle size and PDI are early indicators of instability, such as aggregation and sedimentation (Patravale, Dandekar, and Jain, 2012; Coelho, 2024; Pedrozo, 2023), which was not observed in a relevant manner in this study.

Additionally, the different storage conditions allowed the inference that the nanoemulsion exhibits resistance to both thermal stress and light exposure, although controlled conditions, such as storage in amber glass containers, remain more suitable for preserving the integrity of the bioactive compounds.

**Figure 2 -** Results of the stability analysis regarding nanoparticle size over 90 days and under different storage conditions: amber glass vial protected from light at room temperature (Fig. 2-A), amber glass container in a climatic chamber at ± 35 °C (Fig. 2-B), transparent glass container exposed to light (Fig. 2-C), and amber glass container under refrigeration at - 2 °C (Fig. 2-D).




Statistical analysis was performed using one-way ANOVA followed by Dunnett's post hoc test. Statistically significant differences relative to the NC are indicated by $p < 0.05$ (*), $p < 0.01$ (**), and $p < 0.001$ (***).

The results of the nanoparticle stability analysis over the 90-day storage period demonstrated that the physicochemical stability of the nanoformulation was influenced by the storage conditions. When protected from light in amber glass containers at room temperature, the nanoformulation maintained the hydrodynamic diameter within the range of approximately 120-150 nm, with no significant changes over the storage period and no visible evidence of sedimentation, phase separation, or aggregation. These results indicate that protection from light was effective in maintaining the physical characteristics of the system. In agreement with previous studies, nanoparticulate formulations with particle diameters below 300 nm are generally considered suitable for nanoscale applications, although particle size alone is not sufficient to establish the overall stability of a nanoformulation (Bernardi, 2011; Dallemolea, 2023).

The variations observed in particle size under the different storage conditions may be associated with changes in the particle size distribution and with the physicochemical reorganization of the system throughout storage. Following preparation, nanoemulsions may require a period of stabilization during which the droplets undergo structural adaptation to the surrounding medium. Therefore, measurements performed after this initial stabilization period may provide a more representative assessment of the formulation than measurements obtained immediately after preparation (Pedrozo, 2023). In this context, the variation observed between time zero and subsequent evaluation points does not necessarily indicate progressive destabilization, particularly when the particle size subsequently returns toward values close to the initial measurements.

The condition of light exposure resulted in the most pronounced increase in particle size between 30 and 60 days, reaching approximately 190 nm, followed by a reduction to approximately

130 nm at 90 days. This behavior may be related to the greater susceptibility of lipid components to radiation-induced oxidative processes. In nanoemulsion systems, the high interfacial area associated with the small droplet size may increase the interaction between the oil phase and pro-oxidant species, while exposure to UV radiation may intensify lipid oxidation and consequently alter the physicochemical properties of the droplet interface (Szumała; Wysocka, 2018). Nevertheless, the subsequent reduction in particle size indicates that the increase observed at intermediate storage times does not necessarily represent irreversible destabilization. Rather, it may reflect a transient reorganization of the droplet population during storage. Similar non-linear changes in particle size have been reported in nanoemulsion systems subjected to different environmental stresses, demonstrating that temperature, oil-phase composition, and interfacial properties can influence the mechanisms governing colloidal stability (Liu *et al*., 2021).

A particularly relevant variation was observed under refrigerated storage at - 2 °C, in which the hydrodynamic diameter increased markedly from approximately 140 nm at time zero to approximately 225 nm after 30 days, followed by a progressive reduction to approximately 130 nm at 90 days. This transient increase may be associated with changes in molecular mobility, viscosity, and interfacial equilibrium caused by the low storage temperature. Temperature can influence the physical behavior of nanoemulsions and modify the balance between different destabilization mechanisms. Ghosh *et al.* (2016) demonstrated that storage temperature significantly affects the stability of lipid nanoemulsions, with mechanisms such as Ostwald ripening, flocculation, and coalescence potentially contributing to changes in droplet size depending on the formulation and storage conditions. Therefore, the temporary increase observed at 30 days may reflect a reversible reorganization of the droplets rather than a definitive loss of physical stability.

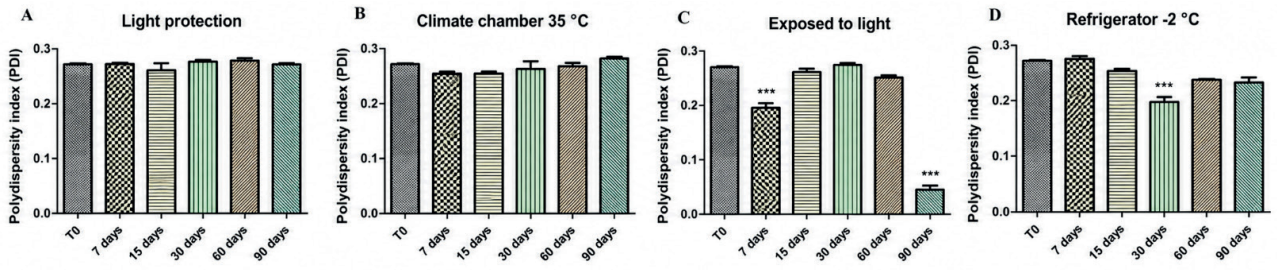
In addition to storage conditions, several formulation and processing parameters can influence the final particle size and its evolution during storage. The production method, concentration and nature of the precursors, oil concentration, temperature, processing time, stabilizing agents, and pH can affect droplet formation, interfacial organization, surface charge, and resistance to aggregation. In formulations containing olive oil, the specific characteristics of the oil, which may vary according to the olive cultivar and extraction method, may also contribute to differences in particle size and stability (Santos, 2023). Thus, the variations observed in the present study should be interpreted as the result of the interaction between formulation characteristics and environmental storage conditions rather than as an effect attributable to a single factor.

It is also important to consider that the particle size measurements were obtained by dynamic light scattering (DLS), which determines the hydrodynamic diameter of particles in suspension and can be particularly sensitive to small populations of larger particles or aggregates. Consequently, temporary increases in the mean hydrodynamic diameter may occur even when the majority of the nanoparticle population remains within the nanoscale range. Therefore, particle size should not be

considered independently when assessing the stability of the nanoformulation. A more comprehensive interpretation should include the polydispersity index (PDI), zeta potential, pH, visual appearance, and other relevant stability parameters. Taken together, the results suggest that protection from light in amber glass provided the most favorable storage condition for maintaining the physicochemical characteristics of the nanoformulation, whereas exposure to light and refrigeration promoted greater fluctuations in particle size during the 90-day period, although these changes were not necessarily indicative of irreversible destabilization.

Figure 3 demonstrates the results obtained from the PDI analysis of the formulations under different storage conditions. According to the studies of Patravale, Dandekar, and Jain, (2012), a fundamental aspect in stability evaluation is the polydispersity index (PDI) of the samples, which should be below 0.3 for the formulation to be considered ideal. This parameter provides insights into the homogeneity of nanoparticle size distribution, indicating that samples with PDI < 0.3 are monodisperse and exhibit a unimodal distribution. In addition to composition, which influences nanoparticle size, the nature of the oil used as the central matrix emerges as a critical factor affecting the polydispersity index. Variations in physical properties, such as viscosity, hydrophobicity, and interfacial tension of the materials employed, have a direct impact on nanoparticle diameter and, consequently, on the PDI value (Patravale, Dandekar, and Jain, 2012).

**Figure 3 -** Results of the stability analysis regarding the polydispersity index of nanoparticles over 90 days and under different storage conditions: amber glass container protected from light (Fig. 3-A), amber glass container in a climatic chamber at ± 35 °C (Fig. 3-B), transparent glass container exposed to light (Fig. 3-C), and amber glass container under refrigeration at - 2 °C (Fig. 3-D).




Statistical analysis was performed using one-way ANOVA followed by Dunnett's post hoc test.
Statistically significant differences relative to the NC are indicated by $p < 0.05$ (*), $p < 0.01$ (**), and $p < 0.001$ (***).

The stability analysis of nanoparticles revealed significant results, demonstrating that storage conditions exert a crucial influence on polydispersity over a period of 90 days. The use of amber glass containers, which protect nanoparticles from light and maintain controlled temperatures, proved to be the most effective strategy to ensure particle stability.

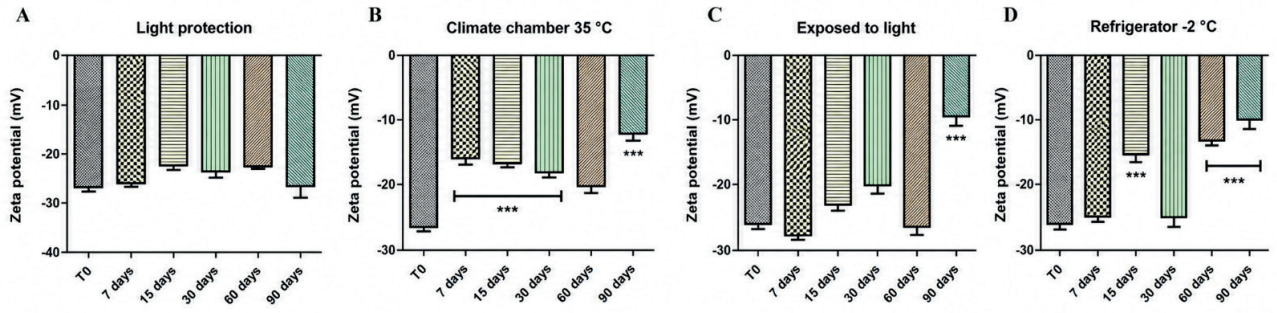
On the other hand, storage in transparent glass containers, which allows light exposure, resulted in more pronounced nanoparticle degradation. This difference highlights the need to implement appropriate storage strategies, as light exposure may not only induce undesirable

reactions but also compromise essential nanoparticle characteristics, such as their efficacy and safety in future applications.

Discussing these results, it becomes clear that proper storage is not merely a matter of convenience, but a fundamental consideration to ensure success in applications that depend on stability. These findings emphasize the importance of protecting nanoparticles from both light radiation and adverse thermal variations, as these conditions may directly affect their physicochemical properties (Carvalho, 2022).

In addition to size and PDI, another parameter to be analyzed is the zeta potential (Figure 4), which reflects the surface potential of nanoparticles, that is, the charge influenced by changes at the interface with the dispersing medium, due to the dissociation of functional groups on the nanoparticle surface or the adsorption of ionic species present in the aqueous medium. When the zeta potential is high, repulsive forces predominate over London attractive forces, causing the droplets to remain dispersed in the system; when the zeta potential is low, attractive forces predominate over repulsive forces, favoring particle approximation and potentially resulting in instability of the preparation. According to the literature, electrostatic repulsion between particles should be close to ±30 mV; therefore, monitoring and optimizing the zeta potential are essential for the development of effective nanometric systems, especially in applications requiring high stability and homogeneity, such as pharmaceutical formulations, cosmetics, and composite materials. Furthermore, manipulation of the zeta potential may represent a valuable strategy for adjusting nanoparticle properties to meet specific requirements in industrial and scientific applications (Patravale, Dandekar, and Jain, 2012; Machado *et al* 2019).

**Figure 4 -** Results of the stability analysis regarding the zeta potential of nanoparticles over 90 days and under different storage conditions: amber glass container protected from light (Fig. 4-A), amber glass container in a climatic chamber at ± 35 °C (Fig. 4-B), transparent glass container exposed to light (Fig. 4-C), and amber glass container under refrigeration at - 2 °C (Fig. 4-D).




Statistical analysis was performed using one-way ANOVA followed by Dunnett's post hoc test. Statistically significant differences relative to the NC are indicated by $p < 0.05$ (*), $p < 0.01$ (**), and $p < 0.001$ (***).

The stability analysis of nanoparticles over a period of 90 days reveals the significant influence of storage conditions on zeta potential behavior. The use of amber glass containers, which provides protection against light exposure, proved to be highly effective in maintaining nanoparticle

stability, especially under controlled temperature conditions, around 35 °C. This approach minimized nanoparticle degradation, preserving their desirable properties over time.

Conversely, storage in transparent glass containers exposed the nanoparticles to light, resulting in a significant compromise of stability. Light exposure may induce undesirable photochemical reactions that affect not only the zeta potential but also other structural and functional characteristics of nanoparticles.

In conclusion, the selection of container material and lighting conditions during storage are critical factors for preserving nanoparticle stability. These results have significant implications for the formulation of pharmaceutical and cosmetic products, since the efficacy and safety of these products depend on the integrity of nanoparticles over time.

The zeta potential values of nanoemulsions are negative due to the chemical composition of their components, which include oleic acid. In the present study, the formulation exhibited a zeta potential value of -26.2 mV. According to the literature, zeta potential values within the range of ±30 mV are considered ideal (Godoi *et al*., 2025). As shown in Figures 4-C and 4-D, some zeta potential values of the developed nanoparticles showed significant differences ($p > 0.05$) throughout the storage period. In both storage conditions, the observed alteration consisted of an increase in the zeta potential value, followed by a slight decrease, before returning to a new increase. These oscillations in the analyzed parameters may be associated with the reorganization and adaptation of the molecules (El-Gogary *et al*., 2021).

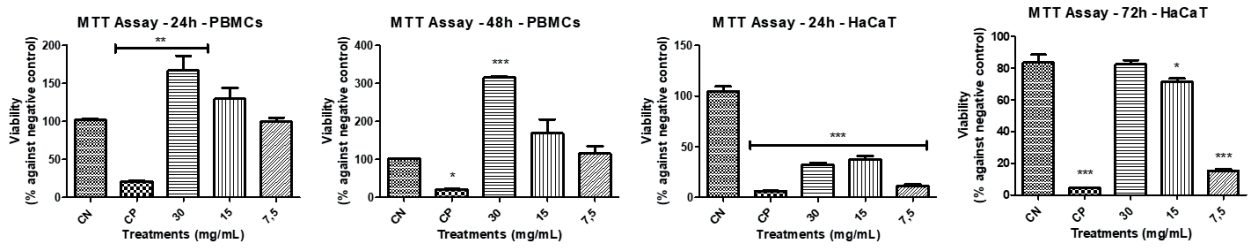
## 3.3 *IN VITRO* BIOCOMPATIBILITY ANALYSIS OF THE NANOEMULSION CONTAINING OLIVE LEAF EXTRACT AND OLIVE OIL

Understanding the biological behavior of nanostructured systems is essential to ensure their safety and efficacy in future pharmacological applications. To obtain a comprehensive analysis of the biocompatibility and therapeutic potential of the developed formulations, *in vitro* assays were conducted using two distinct biological models: peripheral blood mononuclear cells (PBMCs), which allow the investigation of effects on the immune and circulatory systems, and human keratinocytes (HaCaT), a standard model for evaluating interactions with structural cells of connective tissue. Cell viability of the formulations was evaluated using the MTT reduction assay. Hydrogen peroxide ($H_2O_2$) was used as the positive control for cell death, while the negative control significantly decreased cell viability, validating the assay. Analyses were performed at 24 and 48 hours for peripheral blood mononuclear cells (PBMCs) and at 24 and 72 hours for human keratinocytes of the HaCaT cell line, both aiming to evaluate possible acute and delayed toxicity rates.

The evaluation of the cytotoxic potential and biocompatibility of the nanoemulsion containing olive leaf extract and olive oil (NEAZ) against PBMC and human keratinocyte (HaCaT) cellular

models revealed distinct cell viability profiles over time. The results obtained from the MTT reduction assay, expressed as a percentage relative to the negative control, are presented in Figure 5.

**Figure 5 -** Results of the MTT assay at 24 h and 48 h (PBMCs) and 24 h and 72 h (HaCaT) for the nanoemulsion containing olive leaf extract and olive oil (NEAZ), negative control (CN), and positive control (CP).




Data are expressed as mean ± SD and presented as a percentage of the negative control (CN = 100%). Statistical analysis was performed using one-way ANOVA followed by Dunnett's post hoc test. Statistically significant differences relative to the NC are indicated by $p < 0.05$ (*), $p < 0.01$ (**), and $p < 0.001$ (***). CP: positive control ($H_2O_2$).

It can be observed that PBMCs treated with the 30 mg/mL concentration of nanoemulsion for 24 hours showed a significant increase in cell viability (above 150%), indicating proliferation and possibly increased mitochondrial activity, which is highly relevant for the immune system. The concentrations of 15 mg/mL and 7.5 mg/mL remained safe and close to the control. However, after 48 hours of treatment, cell proliferation was even greater, exceeding 300% compared to the control. Studies recognize compounds derived from *Olea europaea* L. as immunomodulators, which may act as mitogenic stimulants, inducing immune cells to enter cell division cycles and consequently increasing proliferation levels (Sánchez, 2020).

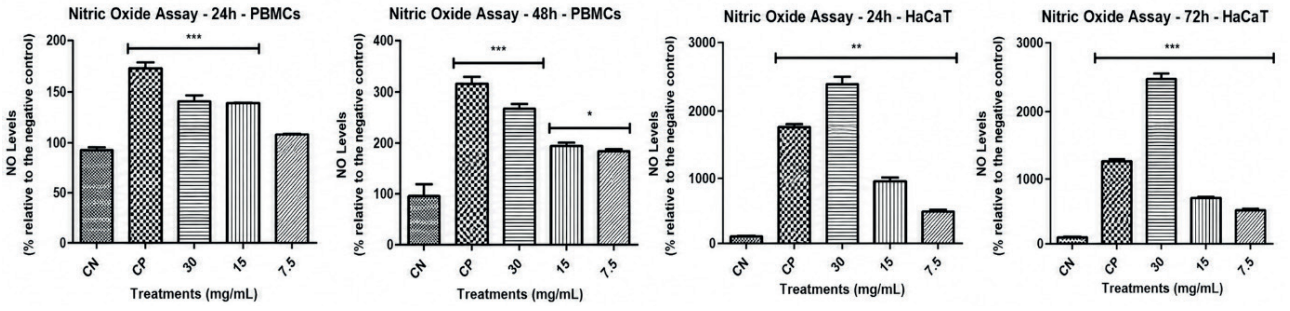
For HaCaT cells, the behavior was completely opposite, with a drastic decrease in cell viability observed at all concentrations. However, at 72 hours, the highest concentrations demonstrated a certain recovery of viability, whereas the 7.5 mg/mL concentration continued to show reduced viability. A possible explanation for this cytotoxic effect at 72 hours may be related to the surfactants/emulsifying agents, which often require higher concentrations to stabilize nanoparticles and, during initial periods and at elevated concentrations in the mg/mL range, may cause solubilization or destabilization of the plasma membrane of cultured cells, generating an immediate acute cytotoxic effect (Arrevolti *et al.*, 2023; Lichtenberg *et al.*, 1983; Maher *et al.*, 2023).

Following the initial shock caused by the surfactant load, within the interval up to 72 hours, an attenuation of this chemical stress may have occurred, either through surfactant degradation in the culture medium, their neutralization by fetal bovine serum proteins, or through cellular metabolism itself. With the reduction of the stressor effect, a temporal window is created for the activation and internalization of phenolic compounds at concentrations of 15 and 30 mg/mL. These bioactive compounds exert their late antioxidant action and stimulate cell proliferation pathways, reversing the initial damage and promoting the expressive increase in viability observed at the end of the period.

In contrast, the lowest concentration may not have been able to reverse the damage, even within this temporal window, due to containing active compounds at concentrations insufficient to exert the same effect as the higher concentrations (Maher *et al.*, 2023).

In view of this scenario of cellular recovery possibly induced by phenolic compounds, we proceeded to investigate the biochemical mechanisms associated with this response, particularly regarding the modulation of oxidative stress and inflammatory signaling. In this context, the analysis of nitric oxide levels emerges as a crucial indicator, since the regulation of this gaseous mediator is directly related to both cytotoxic processes and those involved in cell survival and proliferation (Soares *et al.*, 2015).

**Figure 6 -** Results of the nitric oxide assay at 24 h and 48 h (PBMCs) and 24 h and 72 h (HaCaT) for the nanoemulsion containing olive leaf extract and olive oil (NEAZ), negative control (CN), and positive control (CP).




Data are expressed as mean ± SD and presented as a percentage of the negative control (CN = 100%). Statistical analysis was performed using one-way ANOVA followed by Dunnett's post hoc test. Statistically significant differences relative to the NC are indicated by $p < 0.05$ (*), $p < 0.01$ (**), and $p < 0.001$ (***). CP: positive control ($H_2O_2$).

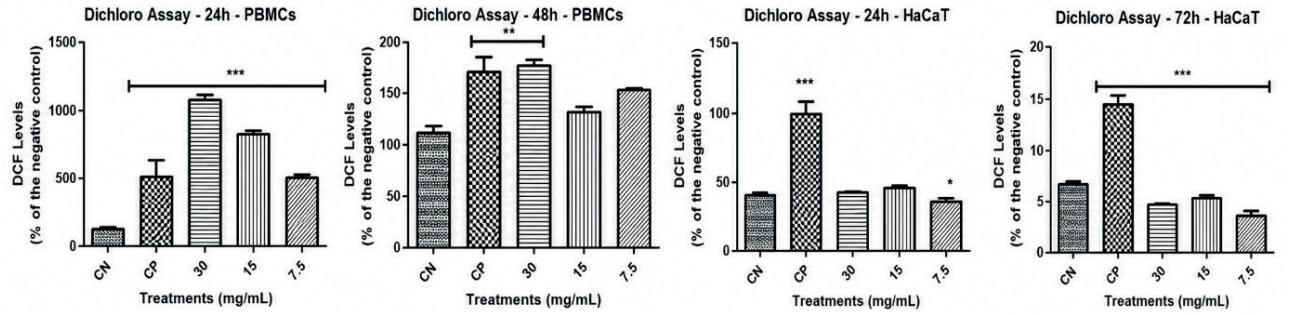
As can be observed in Figure 6, the positive control induced a significant increase in nitric oxide levels in both cell lines, thereby mimicking a severe inflammatory state, validating the assay. In contrast, treatments at 24 and 48 hours were able to attenuate nitric oxide levels, suggesting a late antioxidant action, with the ability to neutralize free radicals and consequently contain the inflammatory cascade in PBMCs, illustrating a time-dependent effect.

When evaluating the treatments in HaCaT cells, it was observed that the highest concentration caused a drastic increase in nitric oxide production, suggesting that the treatments in this epithelial cell line may have initially acted as a pro-oxidant or even cytotoxic agent. The concentrations of 15 and 7.5 mg/mL, at both time points, demonstrated a possible cytoprotective effect, with a drastic reduction in expression, characterizing a concentration-dependent behavior.

Although nitric oxide plays a central role in cellular signaling and cutaneous inflammatory processes, a comprehensive understanding of the antioxidant potential of nanoemulsions requires the evaluation of other reactive oxygen species (ROS) generated in the cellular environment. In this context, the quantification of total intracellular free radicals was performed using the fluorescent probe 2',7'-dichlorodihydrofluorescein diacetate (DCFH-DA) (Figure 7). This assay allowed the investigation of whether the developed formulation is capable of broadly modulating oxidative stress,

complementing the findings obtained for NO and providing a more robust overview of cellular protection and its role in wound-healing activity (Everton, 2025).

**Figure 7 -** Results of the dichlorofluorescein assay at 24 h and 48 h (PBMCs) and 24 h and 72 h (HaCaT) for the nanoemulsion containing olive leaf extract and olive oil (NEAZ), negative control (CN), and positive control (CP).




Data are expressed as mean ± SD and presented as a percentage of the negative control (CN = 100%). Statistical analysis was performed using one-way ANOVA followed by Dunnett's post hoc test. Statistically significant differences relative to the NC are indicated by $p < 0.05$ (*), $p < 0.01$ (**), and $p < 0.001$ (***). CP: positive control ($H_2O_2$).

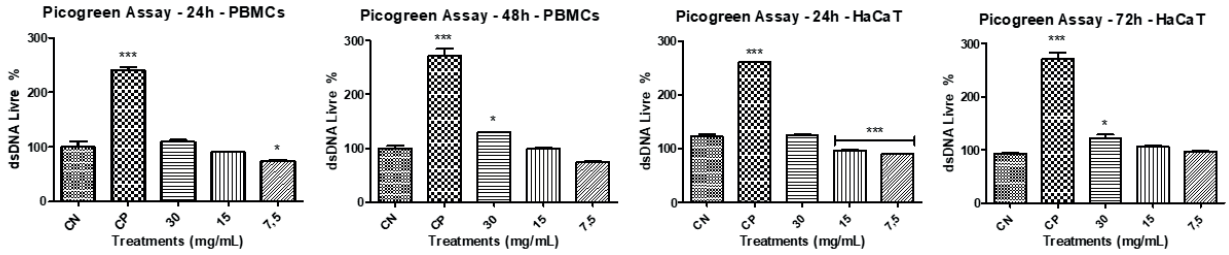
As observed in Figure 7, PBMCs treated for 24 hours with the highest concentration of the formulation exhibited a significant increase in oxidative stress. At concentrations of 15 and 7.5 mg/mL, an increase was also observed, although to a moderate extent. Overall, this profile was concentration-dependent, with lower concentrations generating less stress. This behavior corroborates recent findings in the literature, demonstrating that natural bioactive compounds frequently induce the production of reactive oxygen species (ROS) in peripheral immune cells in a strictly concentration-dependent manner.

At 48 hours, the increase in oxidative stress was maintained, but at levels lower than those observed in the previous period, suggesting an initial acute response with a tendency toward reduction over time. This temporal attenuation suggests a possible late activation of endogenous antioxidant defense mechanisms in PBMCs, modulating the initial stress to restore cellular homeostasis after the acute stimulus (Banzato, 2018; Romeiro *et al*., 2022).

In contrast, keratinocytes (HaCaT) demonstrated a significant reduction in dichlorofluorescein levels, reflecting a decrease in reactive oxygen species. At 24 hours, the concentrations of 30 and 15 mg/mL maintained basal oxidation levels close to the negative control (NC), whereas the lowest concentration (7.5 mg/mL) promoted a statistically significant reduction compared to NC. After 72 hours, this cytoprotective profile became even more pronounced, with all tested concentrations maintaining DCF levels significantly below the positive control (PC). This time- and concentration-dependent response highlights the antioxidant and protective potential of the formulation in the cutaneous barrier. This behavior corroborates a study demonstrating how botanical bioactive compounds stimulate endogenous enzymatic systems in keratinocytes to neutralize chronic oxidative stress and preserve cellular homeostasis (Xiao *et al*., 2020).

Since the accumulation of free radicals can cause genotypic damage and apoptosis, the PicoGreen® assay was used to quantify the presence of free cellular DNA in the supernatant, allowing a direct correlation between the possible antioxidant potential previously demonstrated and the preservation of genetic material and cell viability throughout the treatments.

**Figure 8 -** Results of the PicoGreen® assay at 24 h and 48 h (PBMCs) and 24 h and 72 h (HaCaT) for the nanoemulsion containing olive leaf extract and olive oil (NEAZ), at concentrations equivalent to the MIC (30, 15, and 7.5 mg/mL), negative control (C-), and positive control (C+).




Data are expressed as mean ± SD and presented as a percentage of the negative control (CN = 100%). Statistical analysis was performed using one-way ANOVA followed by Dunnett's post hoc test. Statistically significant differences relative to the NC are indicated by $p < 0.05$ (*), $p < 0.01$ (**), and $p < 0.001$ (***). CP: positive control ($H_2O_2$).

As observed in Figure 8, the results of the PicoGreen® assay demonstrate biocompatibility profiles dependent on cell type, concentration, and exposure time. During the first 24 hours, both cell lines showed excellent tolerability to the tested concentrations, maintaining controlled levels of free dsDNA. In PBMCs, the lower concentrations promoted a statistically significant reduction compared to the negative control, suggesting an initial protective effect. However, at more advanced biological time points, 48 hours for PBMCs and 72 hours for HaCaT, the highest concentration corresponding to the MIC (30 mg/mL) induced a slight but statistically significant increase in extracellular DNA release in both models, indicating the threshold of time-dependent cytotoxicity. In contrast, the concentrations of 15 and 7.5 mg/mL remained strictly safe and at basal levels throughout the entire experimental period in both cell types, confirming the viability and safety of these concentrations for prolonged applications.

## 4 CONCLUSIONS

Based on the results obtained, the nanoemulsion containing olive leaf extract and olive oil proved to be stable, homogeneous, and suitable regarding its physicochemical properties, exhibiting a nanometric-scale diameter, low polydispersity index, negative zeta potential, and slightly acidic pH. Additionally, stability analyses indicated that formulations stored at room temperature and protected from light exhibited higher stability, showing no significant changes in any of the evaluated parameters.

Regarding pharmacological safety and biocompatibility (assessed via MTT, PicoGreen®, nitric oxide, and ROS assays), the nanoformulations demonstrated high biocompatibility and low

cytotoxicity in PBMCs and HaCaT keratinocytes (at concentrations ranging from 30 to 7.5 mg/mL), maintaining cell viability and proliferation without inducing DNA damage, oxidative stress, or inflammatory responses.

Taken together, these findings confirm the safe biological profile of the nanoformulations, consolidating their high potential for topical application as a promising, effective, and innovative alternative for wound healing and skin regeneration.

## ACKNOWLEDGMENTS

I would like to thank the Franciscan University for the infrastructure provided for the development of this research; the company Don José, for their trust, support, and funding of my doctoral studies; my advisors, for their teachings, guidance, and encouragement; and my collaborating colleagues, for their support and contribution to the development of this work.

## REFERENCES

ALVES, S. P. L. *et al*. Avaliação da citotoxicidade in vitro do óleo fixo de Syagrus coronata (Mart.) Becc e do composto majoritário ácido láurico. **Cuadernos de Educación y Desarrollo**, [S. l.], v. 18, n. 1, e10488, 2026. DOI: https://doi.org/10.55905/cuadv18n1-016.

ARREVOLTI, M. *et al*. Cuidado cutâneo através do uso de dermocosméticos nas toxicidades dermatológicas associadas às terapias antineoplásicas. Ponta Grossa: Atena Editora, 2026. cap. 14. DOI: https://doi.org/10.22533/at.ed.1101126130114.

BANZATO, T. P. **Atividade anticâncer e anti-inflamatória da própolis vermelha e de seus compostos bioativos**: anticancer and anti-inflammatory activity of red propolis and its bioactive compounds. 2018. 149 f. Tese (Doutorado em Biologia) - Instituto de Biologia, Universidade Estadual de Campinas, Campinas, 2018.

BERNARDI, D. S. **Desenvolvimento de nanoemulsão de óleo de arroz como adjuvante no tratamento de dermatite atópica e psoríase**. 2011. Dissertação (Mestrado em Ciências Farmacêuticas) - Faculdade de Ciências Farmacêuticas de Ribeirão Preto, Universidade de São Paulo, Ribeirão Preto, 2011. DOI: https://doi.org/10.11606/D.60.2011.tde-11042011-140431.

CHAJI, S. *et al*. Nutrient and bioactive fraction content of Olea europaea L. leaves: assessing the impact of drying methods in a comprehensive study of prominent cultivars in Morocco. **Plants**, [S. l.], v. 13, n. 14, art. 1961, 2024. DOI: https://doi.org/10.3390/plants13141961.

COELHO, L. B. **Desenvolvimento e caracterização de nanoemulsão contendo óleo de tucumã (Astrocaryum vulgare Mart.)**. 2024. 58 f. Trabalho de Conclusão de Curso (Graduação em Farmácia) - Faculdade de Ciências Farmacêuticas, Universidade Estadual Paulista "Júlio de Mesquita Filho", Araraquara, 2024.

COSTA, L. T. **Desempenho competitivo da cadeia produtiva do azeite de oliva extravirgem no Rio Grande do Sul**. 2019. 97 f. Dissertação (Mestrado em Agronegócios) - Centro de Estudos e Pesquisas em Agronegócios, Universidade Federal do Rio Grande do Sul, Porto Alegre, 2019.

DALLEMOLE, D. *et al*. Nanocápsulas de núcleo lipídico: preparação, caracterização e aplicações biológicas. **Química Nova**, [S. l.], v. 46, n. 10, p. 983-997, 2023. DOI: https://doi.org/10.21577/0100-4042.20230077.

EL-GOGARY, R. I. *et al*. Oleuropein as a novel topical antipsoriatic nutraceutical: formulation in microemulsion nanocarrier and exploratory clinical appraisal. **Expert Opinion on Drug Delivery**, [S. l.], v. 18, n. 10, p. 1523-1532, 2021. DOI: https://doi.org/10.1080/17425247.2021.1932813.

EVERTON, G. O. **Perfil químico e potencial biotecnológico antioxidante e anticancerígeno de nanoemulsões (O/A) dos óleos essenciais de Citrus limon (L.) Burn, Cymbopogon citratus (DC) Stapf e Citrus sinensis (L.) Osbeck**. 2025. 92 f. Tese (Doutorado em Química) - Programa de Pós-Graduação em Química, Universidade Federal do Maranhão, São Luís, 2025.

FATHI, M.; MOZAFARI, M. R.; MOHEBBI, M. Nanoencapsulation of food ingredients using lipid based delivery systems. **Trends in Food Science & Technology**, [S. l.], v. 23, n. 1, p. 13-27, 2012. DOI: https://doi.org/10.1016/j.tifs.2011.08.003.

FERREIRA, L. N. *et al*. Gestão multicritério da qualidade na olivicultura: avaliação de propriedades do sudeste e sudoeste Rio-Grandense. **Observatório de la Economía Latinoamericana**, [S. l.], v. 22, n. 6, e5415, 2024. DOI: https://doi.org/10.55905/oelv22n6-207.

GHOSH, S. *et al*. Physicochemical properties and oxidative stability of fish oil nanoemulsions as affected by hydrophilic lipophilic balance, surfactant to oil ratio and storage temperature. **Colloids and Surfaces A**: Physicochemical and Engineering Aspects, [S. l.], v. 506, p. 821-832, 2016.

GODOI, S. N. *et al*. Açaí-loaded nanoemulsion: synthesis, characterization, and in vitro safety profile. **Applied Sciences**, [S. l.], v. 15, n. 16, art. 8822, 2025. DOI: https://doi.org/10.3390/app15168822.

GRAVÁN, P. *et al*. Lipid-core nanoparticles: classification, preparation methods, routes of administration and recent advances in cancer treatment. **Advances in Colloid and Interface Science**, [S. l.], v. 314, art. 102871, 2023. DOI: https://doi.org/10.1016/j.cis.2023.102871.

HERRERO, M. *et al*. New possibilities for the valorization of olive oil by-products. **Journal of Chromatography A**, [S. l.], v. 1218, n. 42, p. 7511-7520, 2011. DOI: https://doi.org/10.1016/j.chroma.2011.04.053.

HUAMÁN-CASTILLA, N. L. *et al*. Comparative analysis of sustainable extraction methods and green solvents for olive leaf extracts with antioxidant and antihyperglycemic activities. **Antioxidants**, [S. l.], v. 13, n. 12, art. 1523, 2024. DOI: https://doi.org/10.3390/antiox13121523.

KABBASH, E. M. *et al*. Comparative metabolic profiling of olive leaf extracts from twelve different cultivars collected in both fruiting and flowering seasons. **Scientific Reports**, [S. l.], v. 13, art. 612, 2023. DOI: https://doi.org/10.1038/s41598-022-27119-5.

LICHTENBERG, D.; ROBSON, R. J.; DENNIS, E. A. Solubilization of phospholipids by detergents: structural and kinetic aspects. **Biochimica et Biophysica Acta - Reviews on Biomembranes**, [S. l.], v. 737, n. 2, p. 285-304, 1983. DOI: https://doi.org/10.1016/0304-4157(83)90004-7.

LIU, M. *et al*. Effect of environmental stresses on physicochemical properties of ALA oil-in-water nanoemulsion system prepared by emulsion phase inversion. **Food Chemistry**, [S. l.], v. 343, art. 128475, 2021. DOI: https://doi.org/10.1016/j.foodchem.2020.128475.

MAHER, S.; GEOGHEGAN, C.; BRAYDEN, D. J. Safety of surfactant excipients in oral drug formulations. **Advanced Drug Delivery Reviews**, [S. l.], v. 202, art. 115086, 2023. DOI: https://doi.org/10.1016/j.addr.2023.115086.

MELLO, L. D.; PINHEIRO, M. F. Aspectos físico-químicos de azeites de oliva e de folhas de oliveira provenientes de cultivares do RS, Brasil. **Alimentos e Nutrição**, Araraquara, v. 23, n. 4, p. 537-548, 2012.

MOSMANN, T. Rapid colorimetric assay for cellular growth and survival: application to proliferation and cytotoxicity assays. **Journal of Immunological Methods**, [S. l.], v. 65, n. 1-2, p. 55-63, 1983. DOI: https://doi.org/10.1016/0022-1759(83)90303-4.

NUNES, M. A. *et al*. Valorization of olive pomace by a green integrated approach applying sustainable extraction and membrane-assisted concentration. **Science of the Total Environment**, [S. l.], v. 652, p. 40-47, 2019. DOI: https://doi.org/10.1016/j.scitotenv.2018.10.204.

OTONI, C. G.; AZEREDO, H. M. C. Nanoemulsões poliméricas. *In*: **Nanotecnologia aplicada a polímeros**. São Paulo: Blucher, 2023. p. 171-196.

PATRAVALE, V.; DANDEKAR, P.; JAIN, R. **Nanoparticulate drug delivery**: perspectives on the transition from laboratory to market. Cambridge: Woodhead Publishing, 2012.

PEDROZO, T. S. **Desenvolvimento e caracterização de nanoemulsão com extrato de cúrcuma por método de baixa energia**. 2023. Trabalho de Conclusão de Curso (Graduação) - Faculdade de Tecnologia de Diadema "Luigi Papaiz", Diadema, 2023.

PENNISI, R. *et al*. Analysis of antioxidant and antiviral effects of olive (Olea europaea L.) leaf extracts and pure compound using cancer cell model. **Biomolecules**, [S. l.], v. 13, n. 2, art. 238, 2023. DOI: https://doi.org/10.3390/biom13020238.

PERISSINATO, A. G. **Desenvolvimento de nanoemulsões biocompatíveis como sistema de liberação intraocular do celecoxibe**. 2019. Tese (Doutorado em Ciências Farmacêuticas) - Faculdade de Ciências Farmacêuticas, Universidade Estadual Paulista, Araraquara, 2019.

PIERRE, M. B. R. Revolução nano: como os sistemas nanométricos estão transformando a liberação cutânea de fármacos. **Revista Faz Ciência**, [S. l.], v. 26, n. 43, p. 50-70, 2024. DOI: https://doi.org/10.48075/rfc.v26i43.31268.

RAPACKI, C. **Métodos de extração de compostos fenólicos do bagaço da oliva**: uma revisão da literatura. [S. l.: s. n.], 2022.

RIEDHAMMER, C.; HALBRITTER, D.; WEISSERT, R. Peripheral blood mononuclear cells: isolation, freezing, thawing, and culture. **Methods in Molecular Biology**, [S. l.], v. 1304, p. 53-61, 2016. DOI: https://doi.org/10.1007/7651_2014_99.

ROMEIRO, C. F. R.; PANTOJA, L. V. P. S.; ANDRADE, M. A. Compostos bioativos identificados em Ayapana triplinervis: uma revisão sobre mecanismos antitumorais. **Research, Society and Development**, [S. l.], v. 11, n. 6, e0811628478, 2022. DOI: https://doi.org/10.33448/rsd-v11i6.28478.

SAGRILLO, M. R. *et al*. Tucumã fruit extracts (Astrocaryum aculeatum Meyer) decrease cytotoxic effects of hydrogen peroxide on human lymphocytes. **Food Chemistry**, [S. l.], v. 173, p. 741-748, 2015. DOI: https://doi.org/10.1016/j.foodchem.2014.10.067.

SÁNCHEZ, M. R. T. **Efecto protector del aceite de oliva sobre la activación de la microglía**. 2020. Tesis (Doctoral) - Universidad de Sevilla, Sevilla, 2020.

SANTOS, A. C. *et al*. **Nanotechnology-based formulations for cutaneous applications**: from theory to clinical practice. [S. l.: s. n.], 2023.

SANTOS, S. **Potencial tecnológico e nutricional das folhas de Moringa oleifera**: variação da região de cultivo, sazonalidade e estádio de maturação. 2020. Dissertação (Mestrado em Tecnologia de Processos Químicos e Bioquímicos) - Universidade Tecnológica Federal do Paraná, Pato Branco, 2020.

SILVA, M. A. **Avaliação in vitro da atividade linfoproliferativa do metil galato frente a células mononucleares do sangue periférico (PBMC) de pacientes com leishmaniose cutânea**. [S. l.: s. n.], 2025.

SOARES, E. D. R. *et al*. Compostos bioativos em alimentos, estresse oxidativo e inflamação: uma visão molecular da nutrição. **Revista Hospital Universitário Pedro Ernesto**, [S. l.], v. 14, n. 3, p. 64-72, 2015. DOI: https://doi.org/10.12957/rhupe.2015.19942.

SZUMAŁA, P.; WYSOCKA, I. Effect of gelation and storage conditions on the oxidative stability of microemulsion and nanoemulsion delivery systems. **European Journal of Pharmaceutical Sciences**, [S. l.], v. 124, p. 17-25, 2018. DOI: https://doi.org/10.1016/j.ejps.2018.08.021.

TALHAOUI, N. *et al*. Phenolic compounds in olive leaves: analytical determination, biotic and abiotic influence, and health benefits. **Food Research International**, [S. l.], v. 77, p. 92-108, 2015. DOI: https://doi.org/10.1016/j.foodres.2015.09.011.

XIAO, Z. *et al*. Trehalose against UVB-induced skin photoaging by suppressing MMP expression and enhancing procollagen I synthesis in HaCaT cells. **Journal of Functional Foods**, [S. l.], v. 74, art. 104198, 2020. DOI: https://doi.org/10.1016/j.jff.2020.104198.